Available online at www.sciencedirect.com
SCIENCE DIRECT®
Bioorganic & Medicinal Chemistry 13 (2005) 4777–4788
Bioorganic & Medicinal Chemistry

# Eugenol and its structural analogs inhibit monoamine oxidase A and exhibit antidepressant-like activity

Guoxin Tao,[a] Yoshifumi Irie,[b] Dian-Jun Li[a] and Wing Ming Keung[a,*]

[a]*Department of Pathology and Center for Biochemical and Biophysical Sciences and Medicine, Harvard Medical School, 77 Avenue Louis Pasteur, Boston, MA 02115, USA*
[b]*Department of Oriental Medicine, Keio University School of Medicine, 35 Shinano-machi, Shinjuku, Tokyo 160-8582, Japan*

Received 12 November 2004; accepted 29 April 2005
Available online 3 June 2005

**Abstract**—Eugenol (**1**) is an active principle of *Rhizoma acori graminei*, a medicinal herb used in Asia for the treatment of symptoms reminiscent of Alzheimer's disease (AD). It has been shown to protect neuronal cells from the cytotoxic effect of amyloid β peptides (Aβs) in cell cultures and exhibit antidepressant-like activity in mice. Results from this study show that eugenol inhibits monoamine oxidase A (MAOA) preferentially with a $K_i$ = 26 μM. It also inhibits MAOB but at much higher concentrations ($K_i$ = 211 μM). In both cases, inhibition is competitive with respect to the monoamine substrate. Survey of compounds structurally related to eugenol has identified a few that inhibit MAOs more potently. Structure activity relationship reveals structural features important for MAOA and MAOB inhibition. Molecular docking experiments were performed to help explain the SAR outcomes. Four of these compounds, two (**1**, **24**) inhibiting MAOA selectively and the other two (**19**, **21**) inhibiting neither MAOA nor MAOB, were tested for antidepressant-like activity using the forced swim test in mice. Results suggest a potential link between the antidepressant activity of eugenol and its MAOA inhibitory activity.


## 1. Introduction

Senile dementia is an acquired global impairment of intellect, memory, and personality, but not of consciousness.[1] Alzheimer's disease (AD) is the most common cause of dementia, accounting for more than 60% of all cases.[2] In the absence of an effective treatment, prevalence of AD is set to increase very rapidly owing to the fast-growing elderly population.[3,4] Thus, effective agents that could prevent, improve, or otherwise ameliorate AD and/or its debilitating symptoms are sorely needed. The etiology of AD is complex as multiple factors could contribute to its pathogenesis. Thus, numerous treatment strategies for AD are being pursued.[5–7] While all these approaches have scientific merits, they have yet to yield major clinical success.

For millennia, herbal remedies have been used in Asia for the treatment of symptoms reminiscent of AD such as deterioration of memory and cognitive function, depression, disinhibitory tendencies, and anxiety. Literature research of ancient Chinese pharmacopoeias revealed that most herbal remedies indicated for AD (or symptoms reminiscent of AD) contain the botanical *Rhizoma acori graminei* (RAG). On the basis of this historical backdrop, we began a systematic investigation of RAG to identify the scientific basis for the traditional use of RAG for the treatment of AD and molecular basis for new drug discovery.

Recently, we reported that a crude extract of RAG is able to protect PC-12 cells from the cytotoxic effect of amyloid β peptides (Aβs),[8] a family of 39–43 amino acid peptides thought to be involved in the pathogenesis of AD.[9] Moreover, we have isolated and identified eugenol (4-allyl-2-methoxyphenol, **1**) from the volatile oil fraction of RAG as its major active principle (Chart 1). The *cis*-2,4,5-trimethoxy-1-propenylbenzene (β-asarone, **5**), another major ingredient of RAG, also protects PC-12 cells from Aβ-induced cell death, but at much higher concentrations. Both eugenol and β-asarone inhibit $Ca^{2+}$ intake by PC-12 cells. While β-asarone mainly inhibits basal $Ca^{2+}$ intake in PC-12 cells, eugenol blocks Aβ-induced $Ca^{2+}$ intake preferentially. Although inconclusive, these results are consistent with the experiences

*Keywords*: Eugenol; MAO inhibitor; Antidepressant.
* Corresponding author. Tel.: +1 617 432 6581; fax: +1 617 432 6580; e-mail: wingming_keung@hms.harvard.edu

0968-0896/$ - see front matter © 2005 Elsevier Ltd. All rights reserved.
doi:10.1016/j.bmc.2005.04.081

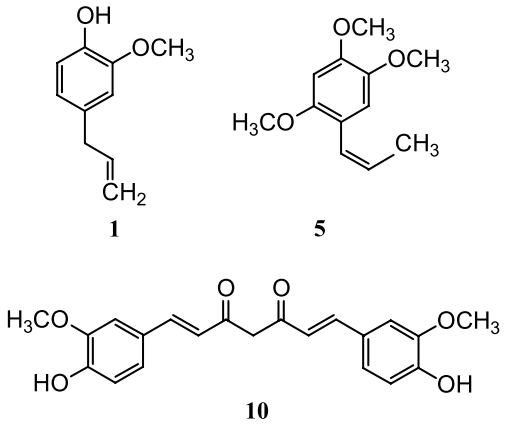


**Chart 1.** Chemical structures of eugenol (**1**), β-asarone (**5**), and curcumin (**10**).

recorded in ancient Chinese pharmacopoeias and support the notion that RAG and one or more of its active principles may be new leads for the development of effective prophylactic and/or therapeutic agents for AD.

Depression is one of the most prevalent neuropsychiatric comorbidities of AD. Up to 50% of all patients suffer from some form of depression.[10] It is associated with serious negative consequences for patients and their caregivers. Yet, available studies on the treatment of depression associated with AD have been few and equivocal.[10–12] As a continuing effort to delineate the potential pharmacological efficacies of RAG, we tested eugenol for potential antidepressant-like activity in mice using two established screening tests: the tail suspension test (TST) and the forced swim test (FST). The results, reported in a recent communication, show that eugenol, administered as a solute in drinking water, exhibits an antidepressant-like activity in mice comparable to that of imipramine, the classical tricyclic antidepressant (TCA).[13]

Since the debut of TCAs, the nonspecific blockers of monoamine uptake, new classes of antidepressants have been developed and approved for the treatment of depression. These include the selective serotonin reuptake inhibitors (SSRIs), serotonin and norepinephrine reuptake inhibitors (SNRIs), the nonselective and irreversible inhibitors of MAOA and MAOB, and the selective and reversible inhibitors of MAOA (RIMAs).[10] In the present study, we have tested the effect of eugenol on the catalytic activity of MAOs and have shown that eugenol inhibits MAOA preferentially with a $K_i$ = 26 μM. It also inhibits MAOB but at much higher concentrations ($K_i$ = 211 μM). Further, we have examined commercially available compounds structurally related to eugenol and revealed a potential link between its MAOA inhibitory activity and antidepressant-like activity. The selectivity of MAOA versus MAOB inhibition by eugenol and its structural analogs was evaluated in light of the recently published 3D structures of MAOA and MAOB.[14–17] Information obtained from these studies could be useful for the design of more potent and selective inhibitors for MAOA and MAOB.

## 2. Results and discussion

### 2.1. Eugenol inhibits human MAOA and MAOB

Eugenol inhibits human MAOA (Fig. 1, solid circle). The $IC_{50}$ value determined at 10 μM 5-HT, a specific substrate of MAOA, is 34.4 μM. While the activity of human recombinant MAOB was also inhibited by eugenol, it was less sensitive than MAOA (Fig. 1, open circle). Its $IC_{50}$ value, determined at 10 μM DA, is 288 μM.

The kinetics of eugenol inhibition of human MAOA and MAOB was studied using initial velocity method under one atmospheric air. The kinetic parameters obtained for MAOA and MAOB are shown in Table 1 and the data from which they were derived in Figure 2. In the absence of eugenol, the apparent $K_m$'s of 5-HT and DA for MAOA and MAOB are 192 μM and 230 μM, respectively; similar to those reported for the MAOA (137 μM and 178 μM) and MAOB (229 μM) activities in the homogenates of human cerebral cortex.[18,19] Eugenol inhibits human MAOA and MAOB competitively with respect to 5-HT and DA, respectively. The apparent $K_i$ values determined under these conditions are 26 and 211 μM for MAOA and MAOB, respectively. In both cases, eugenol inhibition is reversible. In the presence of 100 μM eugenol, human MAOA and MAOB activities were inhibited by about 80% and 35%, respectively. A 100-fold dilution of the inhibited enzymes in eugenol free assay medium restored both activities to about 98% of their controls (result not shown).

In a recent study, Kong et al.[20] have examined seventeen phytochemicals including eugenol for inhibitory activity

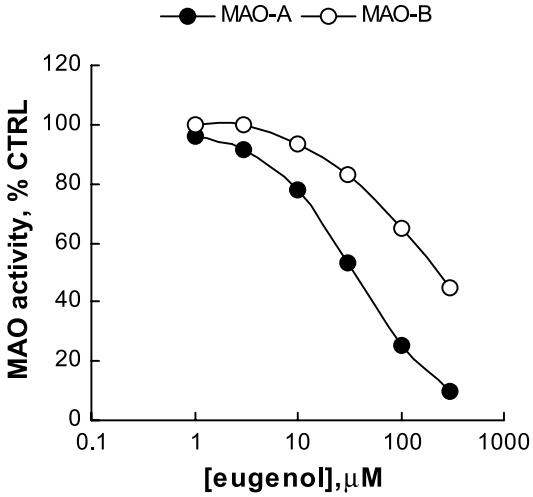


**Figure 1.** Inhibition of human MAOA (solid circles) and MAOB (open circles) by eugenol (see Section 4 for enzyme assay conditions).

**Table 1.** Kinetic parameters of human recombinant MAOA and MAOB towards 5-HT and DA as substrates, respectively, assayed at pH 7.4 under an atmosphere of air

| Isozyme | $K_m$ (μM) | $K_i$ (eugenol, μM) |
|---|---|---|
| MAOA | 192 (5-HT) | 26 |
| MAOB | 230 (DA) | 211 |

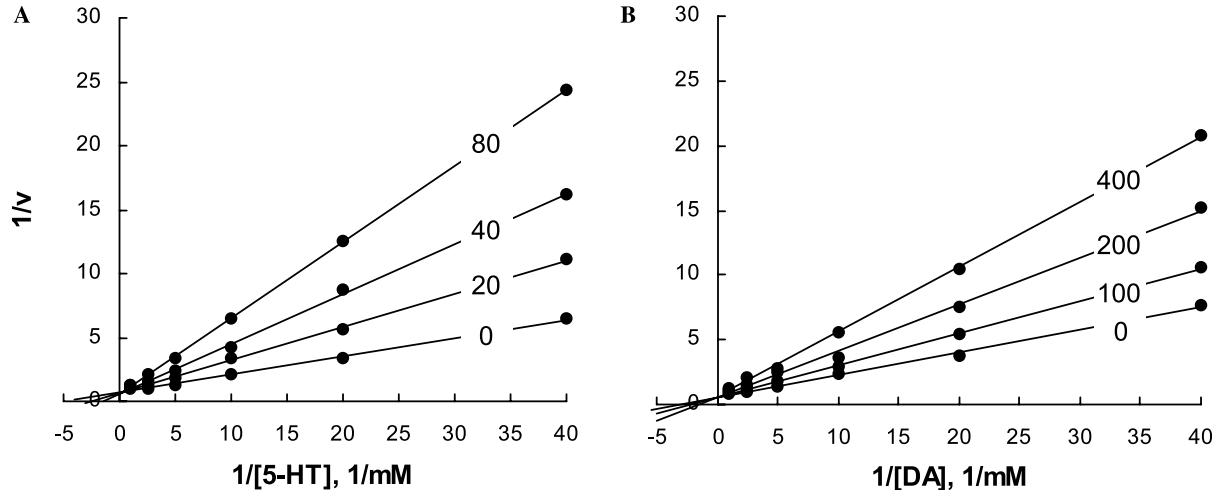


**Figure 2.** Double reciprocal plot of eugenol inhibition of human (A) MAOA catalyzed 5-HT deamination, and (B) MAOB catalyzed DA deamination.

toward the MAOA and MAOB activities in a rat brain mitochondrial fraction and shown that eugenol, at concentrations up to 100 μM, inhibited neither MAOA nor MAOB. This conflicting result could be attributed to the high DMSO concentration (5%) in their enzyme assays. DMSO concentration in the assay media of the present study was 0.2%, much lower than that used by Kong et al. (5%). Toward this end, we have studied the effect of DMSO on MAOA activity and its inhibition by eugenol. Results from this study show that MAOA activity observed in 5% of DMSO is only 48% of that determined in 0.2% DMSO. Further, the $IC_{50}$ value of eugenol inhibition of MAOA obtained in 5% DMSO (352 μM) is ten times higher than that determined in 0.2% DMSO (34 μM).

Survey of commercially available compounds structurally related to eugenol identified nineteen that inhibit MAOs (Table 2, not shaded). Like eugenol, most of these analogs inhibit MAOA preferentially with selectivity values ranging from 2.45 (analog **3**) to >49 (analog **2**). Six of the MAOA inhibitory analogs (**11**, **20**, **24**, **31**, **32**, and **39**) do not inhibit MAOB at concentrations up to 500 μM. Among the analogs tested, only **27** and **29** inhibit MAOB more potently than MAOA with selectivity values of 0.66 and 0.23, respectively. In fact, among all the compounds studied only **27** and **29** inhibit MAOB with significant potency. Six of the analogs studied, namely, **2**, **10**, **24**, **27**, **29**, and **39**, are more potent MAOA inhibitors than eugenol.

### 2.2. Eugenol analogs inhibit MAOA and exhibit antidepressant-like activity

The potential antidepressant-like activities of four selected compounds were examined in mice using the forced swim test (FST). Two of them, eugenol (**1**) and **24**, are potent and selective inhibitors of MAOA. The other two, compounds **19** and **21**, have little, if any, inhibitory activity toward either MAOA or MAOB (Table 2). Results from this study show that both eugenol and compound **24** increase the FST scores significantly, whereas compounds **19** and **21** exhibit no effect on the FST scores (Fig. 3).

In a previous study,[13] we have shown that imipramine treated mice registered higher FST scores than the vehicle controls and that eugenol, given by the same route, produced a similar effect. These results were also confirmed with the TST. Results from the present study have again confirmed the imipramine-like antidepressant activity of eugenol. Further, it suggests that the antidepressant activity of eugenol could be attributed to its ability to inhibit MAO as analogs **19** and **21**, which have low or no MAO inhibitory activity, exhibit no antidepressant activity. The fact that the MAOA selective inhibitor analog **24** is as active in the FST as eugenol suggests that MAOA inhibition alone is sufficient for antidepressant activity.

### 2.3. Structure activity relationship

Examination of the structural characteristics of the eugenol analogs revealed that some of them are important for MAOA and/or MAOB inhibition. Perhaps, the most striking feature is the dominant effect of the free carboxyl function. In all cases, introduction of a free carboxyl group either to the aromatic ring as in analogs **6**, **7**, **19**, **23**, **34**, **35**, and **36**, or to the terminal of a ring-substituent as in analogs **8**, **9**, **21**, **22**, and **40**, dramatically decreases the potencies for MAO inhibition (Table 2, shaded). The detrimental effect of the free carboxyl function can be best illustrated by comparing analog **21** (3-hydroxy-4-methoxycinnamic acid) with its ethyl ester analog **29** (3-hydroxy-4-methoxycinnamic acid ethyl ester). While the free acid (**21**) has little ($IC_{50}$ > 500 μM) or no inhibitory activity toward MAOA and MAOB, its ethyl ester (**29**) inhibits both isozymes rather potently with $IC_{50}$ values of 24.7 and 5.7 μM, respectively. This finding suggests that the free carboxyl group, presumably in the form of a carboxyl anion under physiological pH, discourages or prevents these compounds from entering and/or binding to the active sites of both MAOA and MAOB.

**Table 2.** Inhibition of human MAOA and MAOB by eugenol (**1**) and structurally related compounds

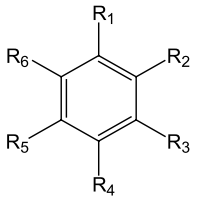


| Compound | R1 | R2 | R3 | R4 | R5 | R6 | $IC_{50}$ (μM) | | Selectivity $IC_{50}$ [(B)/(A)] |
|---|---|---|---|---|---|---|---|---|---|
| | | | | | | | MAOA | MAOB | |
| **1** | OH | $OCH_3$ | H | $CH_2CH{=}CH_2$ | H | H | 34.4 ± 5.1 | 288 ± 47 | 8.37 |
| **2** | OH | $OCH_3$ | H | H | H | $CH_2CH{=}CH_2$ | 10.1 ± 1.8 | >500 | >49 |
| **3** | $OCH_3$ | $OCH_3$ | H | $CH_2CH{=}CH_2$ | H | H | 110 ± 13.3 | 269 ± 34 | 2.45 |
| **4** | $OCH_3$ | $OCH_3$ | H | $CH{=}CHCH_3$ (*trans*) | $OCH_3$ | H | 124 ± 16 | 338 ± 52 | 2.73 |
| **5** | $OCH_3$ | $OCH_3$ | H | $CH{=}CHCH_3$ (*cis*) | $OCH_3$ | H | 142 ± 18 | 362 ± 43 | 2.55 |
| **6** | COOH | $OCH_3$ | H | $OCH_3$ | $OCH_3$ | H | NI[a] | 412 ± 37 | —[b] |
| **7** | COOH | H | $OCH_3$ | $OCH_3$ | $OCH_3$ | H | NI | 425 ± 29 | —[b] |
| **8** | $OCH_3$ | $OCH_3$ | H | CH=CHCOOH (*trans*) | H | $OCH_3$ | >500 | >500 | —[b] |
| **9** | OH | OH | H | CH=CHCOOH (*trans*) | H | H | >500 | >500 | —[b] |
| **10** | See Chart 1 for complete structure | | | | | | 12.3 ± 2.1 | 122 ± 27 | 9.92 |
| **11** | OH | $OCH_3$ | H | $CH_2CH_2OH$ | H | H | 180 ± 24 | NI | —[b] |
| **16** | OH | $OCH_3$ | H | H | H | H | 175 ± 27 | >500 | >2.86 |
| **17** | OH | $OCH_3$ | H | H | H | $OCH_3$ | 62.4 ± 8.6 | >500 | >8.01 |
| **18** | OH | $OCH_3$ | H | $CH_2NH_2$ | H | H | 130 ± 18 | 382 ± 41 | 2.94 |
| **19** | OH | $OCH_3$ | H | H | COOH | H | NI | NI | —[b] |
| **20** | OH | $OCH_3$ | H | $CH_2COCH_3$ | H | H | 30.2 ± 4.7 | NI | —[b] |
| **21** | OH | $OCH_3$ | H | CH=CHCOOH (*trans*) | H | H | >500 | NI | —[b] |
| **22** | OH | $OCH_3$ | H | H | CH=CHCOOH (*trans*) | H | NI | NI | —[b] |
| **23** | COOH | $OCH_3$ | $OCH_3$ | H | H | H | NI | NI | —[b] |
| **24** | OH | $OCH_3$ | H | $CH_2COOCH_2CH_3$ | H | H | 8.1 ± 1.3 | NI | —[b] |
| **27** | OH | $OCH_3$ | H | OH | H | H | 13.4 ± 2.4 | 8.9 ± 1.4 | 0.66 |
| **29** | OH | $OCH_3$ | H | $CH{=}CHCOOCH_2CH_3$(*trans*) | H | H | 24.7 ± 4.3 | 5.7 ± 0.8 | 0.23 |
| **31** | OH | $OCH_3$ | H | $CH(OH)CH_2NHCH_3$ | H | H | 252 ± 31 | NI | —[b] |
| **32** | OH | $OCH_3$ | $OCH_3$ | H | CHO | H | 131 ± 21 | NI | —[b] |
| **34** | COOH | $OCH_3$ | H | H | $OCH_3$ | H | NI | NI | —[b] |
| **35** | COOH | $OCH_3$ | H | H | H | H | NI | NI | —[b] |
| **36** | COOH | $OCH_3$ | H | H | H | $OCH_3$ | NI | NI | —[b] |
| **37** | $NH_2$ | $OCH_3$ | H | $OCH_3$ | H | H | 42 ± 6.2 | 390 ± 48 | 9.29 |
| **38** | $NH_2$ | $OCH_3$ | H | H | $CH_3$ | H | 150 ± 22 | >500 | >3.33 |
| **39** | OH | H | $OCH_3$ | H | H | H | 24 ± 2.8 | NI | —[b] |
| **40** | $CH_2COOH$ | H | H | OH | H | H | NI | NI | —[b] |

[a] NI: no significant inhibition at concentrations up to 500 μM.
[b] Undefined.

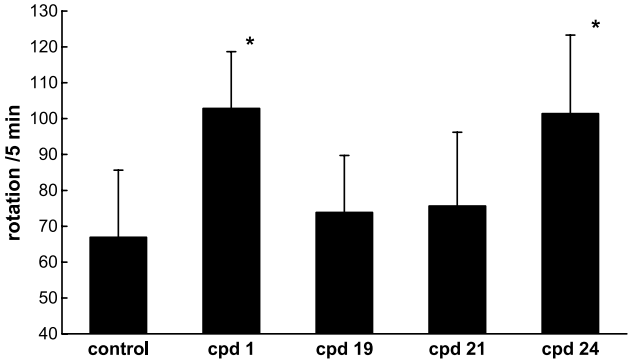


**Figure 3.** Forced swim test (FST) on CD-1 mice after 14-day treatment with eugenol or its analogs (0.17 mmol/day/kg body weight, po). Mice on eugenol (**1**) and ethyl homovanillate (**24**) increased wheel rotation significantly, whereas 3-hydroxy-4-methoxybenzoic acid (**19**) and *trans*-3-hydroxy-4-methoxycinnamic acid (**21**) did not. $N = 8$ for each group. $^{*}P < 0.05$ compared with the control by the Student $t$ test. See Section 4 for details.

The free hydroxyl group of eugenol appears to be important for MAOA but not MAOB inhibition, as replacing it with a methoxy function (**3**) decreases potency for MAOA but not MAOB inhibition (Chart 2). The position of the allyl function of eugenol also appears to affect selectivity, as moving it from the 4 position as in eugenol to the 6 position as in **2** on the phenolic ring increases potency for MAOA (decreases $IC_{50}$ value from 34.4 to 10.1 μM), while it decreases that for MAOB inhibition (increases the $IC_{50}$ value from 288 to >500 μM).

Effect of substituting the allyl function of eugenol on MAOA and MAOB inhibition varies as the nature of the substituent (Chart 3). Replacing it with hydrogen (**16**), 2-hydroxyethyl (**11**), amino (**18**), or 1-hydroxy-2-methylaminoethyl (**31**) group decreases inhibition for both MAOA and MAOB, whereas substituting it with hydroxyl (**27**) or 3-ethoxy-3-oxo-propenyl (**29**) group increases inhibition for both isozymes. Replacing the 4-allyl function of eugenol with 2-oxo-propyl (**20**) or ethoxycarbonylmethyl (**24**) increases selectivity, as both manipulations increase inhibition for MAOA but decrease that for MAOB.

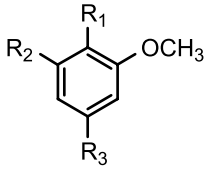


| | | | | $IC_{50}$, μM | | |
|---|---|---|---|---|---|---|
| **Cpd** | **R1** | **R2** | **R3** | **MAO-A** | **MAO-B** | **Selectivity** |
| **1** | -OH | -H |  | 34.4 | 288 | 8.37 |
| **2** | -OH |  | -H | 10.1 | >500 | >49 |
| **3** | $-OCH_3$ | -H |  | 110 | 269 | 2.45 |

**Chart 2.** Structure activity relationship—I.

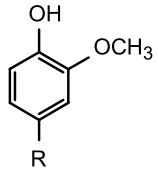


| | | $IC_{50}$, μM | | |
|---|---|---|---|---|
| **Cpd** | **R** | **MAO-A** | **MAO-B** | **Selectivity** |
| **1** |  | 34.4 | 288 | 8.37 |
| **11** |  | 180 | NI | - |
| **16** | −H | 175 | >500 | >2.86 |
| **18** |  | 130 | 382 | 2.94 |
| **20** |  | 30.2 | NI | - |
| **21** |  | >500 | NI | - |
| **24** |  | 8.1 | NI | - |
| **27** | −OH | 13.4 | 8.9 | 0.66 |
| **29** | 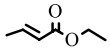 | 24.7 | 5.7 | 0.23 |
| **31** |  | 252 | NI | - |

**Chart 3.** Structure activity relationship—II.

## 2.4. Docking and molecular modeling

To gain further insight into the potential mode of binding of eugenol and its analogs in MAOA and MAOB, and to help explain the SAR outcomes, docking and molecular modeling experiments were performed. Coordinates from crystal structures of MAOs used for molecular docking were retrieved from the Protein Data Bank (PDB). The co-crystal structure of rat MAOA with covalently bound clorgyline (PDB 1O5W) was used in this study because it is the only MAOA structure known.[17] Although the inhibition data reported here were determined using human recombinant MAOA and MAOB, the facts that the primary sequences of human and rat MAOA share 90% identity and that all of the active site residues are conserved in the human and rat enzyme suggest that results obtained from this approach should shed light on the mode of inhibitor binding to the human enzyme. Nevertheless, given the fact that recent studies suggested that residues Phe208 and Ile199 critical in determining substrate and inhibitor specificities in rat MAOA and MAOB, respectively, might not be important in the human enzymes,[21,22] a note of caution is warranted. Docking results reported here should be verified when the crystal structure of human MAOA becomes available.

Ten human MAOB–inhibitor complexes have been deposited in the PDB to date.[14–16] Three are structures with reversibly bound inhibitors: isatin (1OJA), 1,4-diphenyl-2-butene (1OJ9), and lauryldimethylamine-*N*-oxide (1OJD); and seven are with irreversibly bound inhibitors: pargyline (1GOS), *N*-(2-aminoethyl)-*p*-chlorobenzamine (1OJC), tranylcypromine (1OJB), *N*-prop-

argyl-1(*S*)-aminoindan (1S2Y), 6-hydroxy-*N*-propargyl-1(*R*)-aminoindan (1S3E), *N*-methyl-*N*-propargyl-1(*R*)-aminoindan (1S3B), and rasagiline (1S2Q). The structures of isatin–MAOB (1OJA), pargyline–MAOB (1GOS), and 1,4-diphenyl-2-butene-MAOB (1OJ9) were selected for the docking experiments, as they represent the three most distinctive active site conformations, that is, the closed, half-open, and open, observed thus far.[14–16]

### 2.5. Docking eugenol into the inhibitor-binding pocket in clorgyline-MAOA (1O5W) and pargyline–MAOB (1GOS)

Figure 4 illustrates the structure of eugenol docked into the inhibitor-binding pocket of clorgyline-MAOA (Fig. 4a) and pargyline–MAOB (Fig. 4b). Structures of the irreversibly bound clorgyline and pargyline retrieved from the PDB and those of clorgyline and pargyline docked into their respective isozymes are also shown for comparison. Eugenol docked into the 'substrate cavity space' of MAOA outlined by residues Tyr69, Asn181, Tyr197, Tyr407, Gly443, Tyr444, and the isoalloxazine ring (Figs. 4a and 5). A characteristic feature of this mode of binding as opposed to that observed in MAOB (Fig. 4b) is the packing of its methoxyphenol moiety between the phenolic side chains of Tyr407 and Tyr444. These phenols face each other in space with the shortest edge-to-edge distance of 6.7 Å and a dihedral angle of 36°. This geometric arrangement apparently allows partial insertion of the methoxyphenol of eugenol into the space between the phenolic side chains of Tyr407 and Tyr444 so that binding could be enhanced through favorable π–π stacking interaction. A partial π–π stacking interaction might also occur between the phenolic ring of Tyr69 and the allyl double bond of the eugenol molecule. In addition, the 1-OH of eugenol is within H-bonding distances from the backbone carbonyl oxygen of Asn181 and the side chains of Tyr197 and Tyr444. Its methoxy group could also make VDW contacts with the backbone atoms of Tyr407. Together, these interactions might have contributed to the relatively tight binding of eugenol to MAOA ($K_i$ = 26 μM).

Docking eugenol into the inhibitor-binding pocket of pargyline–MAOB revealed a mode of binding (Fig. 4b) different from that observed in MAOA. In MAOB, docked eugenol assumes a binding orientation similar to that of the covalently bound pargyline in which its

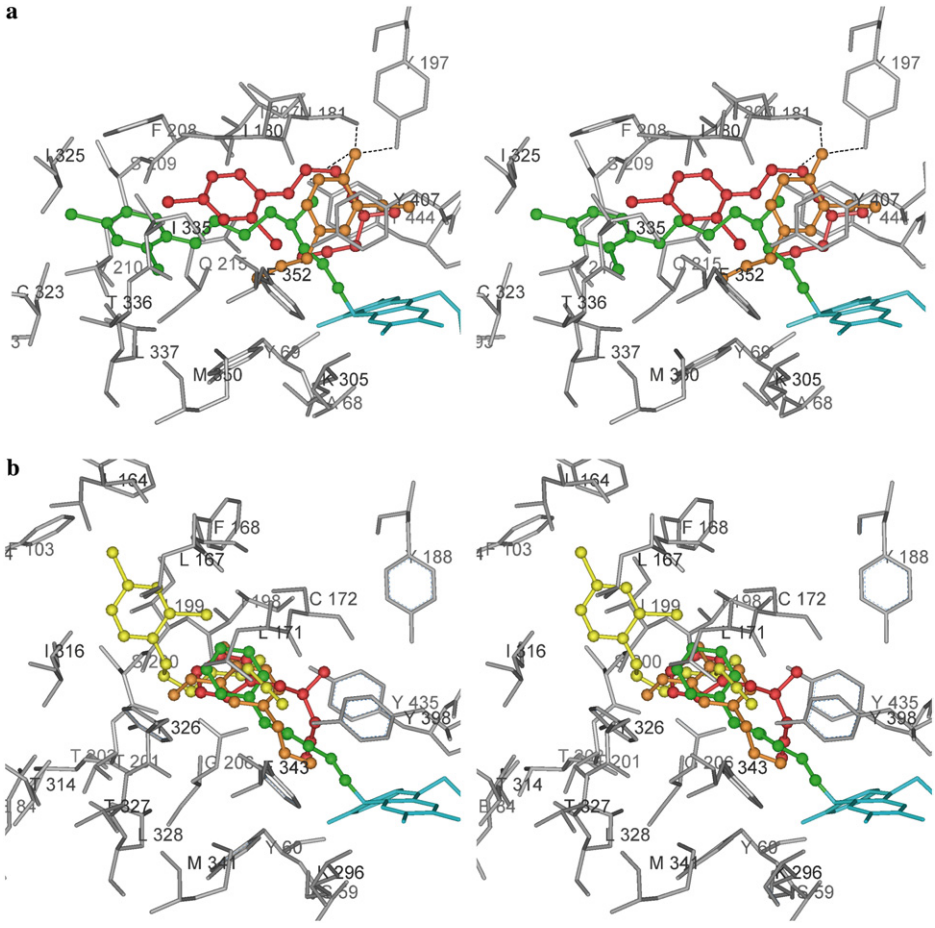


**Figure 4.** Stereo views illustrating the calculated binding modes of (a) eugenol (gold) and clorgyline (red) in the inhibitor binding pocket of MAOA (PDB code 1O5W) with covalently bound clorgyline (green), and (b) eugenol (gold), clorgyline (yellow), and pargyline (red) in the inhibitor binding pocket of MAOB (PDB code 1GOS) with covalently bound pargyline (green). MAOs are in gray stick, isoalloxazine ring is in cyan stick, inhibitors are in color ball-and-stick models, and hydrogen bonds are in black broken lines. Graphics were created using Insight II and docking was performed using AutoDock 3.0.[29]

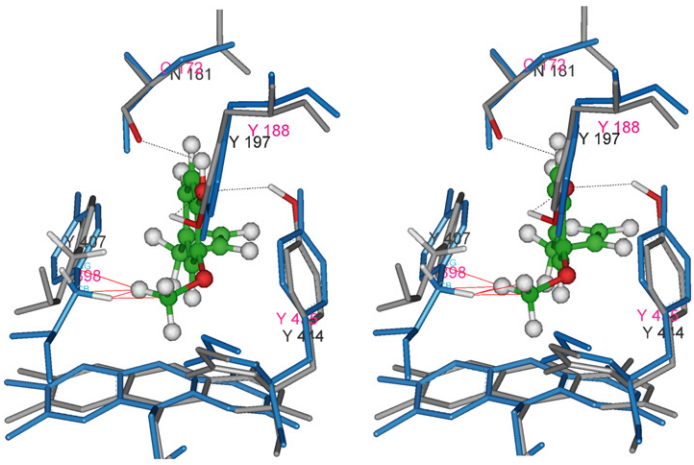


**Figure 5.** Superposition of MAOB on MAOA with eugenol docked in MAOA. Eugenol is in ball-and-stick models and colored according to atom type, red for oxygen, white for hydrogen, and green for carbon. Atoms on MAOA within H-bonding or clashing distance from eugenol are also colored accordingly. Potential H-bonds are shown in black broken lines and clashes are shown in solid red lines. Labels are pink for MAOB and black for MAOA. Graphics were created using Insight II and docking was performed using AutoDock 3.0.[29]

aromatic ring is sandwiched by the side chains of Gln206 and Leu171. Such difference might be attributed to the fact that, unlike MAOA, the phenolic groups of the corresponding Tyr398 and Tyr435 in MAOB are less parallel to each other (dihedral angle $\approx 68°$) and are much closer to each other (shortest edge–edge distance = 6.15Å). Indeed, superposing structures of the inhibitor-binding pocket of MAOB and that of eugenol docked in MAOA (Fig. 5) clearly indicate that the methoxy function of eugenol would have bumped into the side chain of Tyr398 in MAOB. Unable to capitalize from the π–π stacking interaction between methoxyphenol function of eugenol and the phenolic groups of Tyr398 and Tyr435 might have rendered it a much weaker inhibitor for MAOB ($K_i$ = 211 μM).

### 2.6. Docking clorgyline and pargyline into the inhibitor-binding pocket of clorgyline-MAOA (1O5W) and pargyline–MAOB (1GOS)

Significant differences were observed between the mode of binding of the irreversibly (from x-ray structure) and reversibly (predicted by docking) bound clorgyline in MAOA (Fig. 4a), and to a lesser extent, pargyline in MAOB (Fig. 4b). In the irreversible mode, the dichlorophenyl moiety of clorgyline extends from the 'substrate cavity space' into the area corresponding to the 'entrance cavity space' in MAOB as defined by Binda et al.[16] However, docking clorgyline into MAOA yielded a markedly different mode of binding in which the whole clorgyline molecule lodges inside the 'substrate cavity space' with its dichlorophenyl function lodged in the hydrophobic pocket outlined by Ile180, Asn181, Phe208, and Gln215, and the ternary amine portion of its acetylenic side chain sandwiched between the side chains of Tyr407 and Tyr444 (Fig. 4a, red). The $K_i$ of clorgyline for MAOA estimated by AutoDock 3.0 is 12.6 nM.

Superposing the active site structure of MAOB with covalently bound pargyline with that of MAOA with covalently bound clorgyline, Ma et al.[17] has demonstrated that clorgyline would not fit into the inhibitor-binding pocket of MAOB because access to the 'entrance cavity space' is completely blocked by the side chain of Tyr326. However, docking clorgyline into the inhibitor-binding site of pargyline–MAOB yielded a reasonably good, yet different, mode of binding (Fig. 4b). In this case, the dichlorophenyl ring of clorgyline docked into an area between Ile199 and Phe326, whereas its acetylenic side chain packed between the side chains of Leu171 and Gln206. The limited space between the phenolic groups of Tyr398 and Tyr435, and the replacement of the bulky Phe208 in MAOA with a less bulky Ile199 in MAOB could have facilitated relocating the clorgyline-binding pocket farther away from the isoalloxazine ring. Nevertheless, the $K_i$ of docked clorgyline for MAOB (119 nM) is much higher than that for MAOA is consistent with the fact that the instantaneous, reversible inhibition constant of clorgyline for MAOA is much lower than that for MAOB.[23]

The potential mode of binding of reversibly bound pargyline in MAOB predicted by docking is quite similar to that of the irreversibly bound pargyline derived from crystallography studies.[14–16] In both cases, the phenyl group of pargyline is sandwiched by the side chains of Gln 206 and Leu171 (Fig. 4b, red). Like the allyl side chain of eugenol, the acetylenic side chain of pargyline also avoids close contact with the phenolic side chains of Tyr398 and Tyr435, and the isoalloxazine ring.

In this context, it is of interest to note that the reversible binding mode of clorgyline in MAOA (Fig. 4a) and that of pargyline in MAOB predicted by computer docking are likely 'nonproductive,' that is, they do not readily lead to the mechanism-based irreversible inhibition of the respective MAOs.[23,24] One possible explanation is that the active site structures of MAOs with covalently bound inhibitors might have been transformed by a series of chemical manipulations, and therefore, have very different conformations from those of the resting state of

the free enzymes. If this were the case, docking experiments using coordinates from crystal structures of MAOs with irreversibly bound inhibitors such as clorgyline and pargyline would likely yield artifactual results. On the other hand, one can also argue that their 'productive' binding modes that lead to irreversible inactivation might not be the ones that cause the instantaneous, reversible inhibition of the MAOs and have the lowest docked energies. This argument is not totally unfounded given the facts that (i) superposing the structure of pargyline–MAOB (1GOS) to that of isatin–MAOB (1OJA) revealed little structural difference in their substrate binding cavities (not shown), and (ii) docking pargyline into the structure of isatin–MAOB and pargyline–MAOB yielded virtually identical mode of binding (see Fig. 7a).

### 2.7. Docking MAOA inhibitory analogs into the inhibitor-binding pocket of clorgyline-MAOA

All MAOA inhibitory analogs, including those of relatively low potency (Table 2), docked into the inhibitor-binding pocket of clorgyline-MAOA in a similar manner as eugenol, with their substituted aromatic rings packed between the side chains of Tyr407 and Tyr444. This mode of binding is illustrated in Figure 6a using three of the most potent analogs, **2** (blue), **24** (yellow), and **27** (red). Docked eugenol (gold) is also shown for comparison. Like eugenol, docked analogs **2**, **24**, and **27** interact favorably with the phenolic side chains of Tyr407 and Tyr444. Based on the relative docked position and orientation of their aromatic rings, that of analog **27** should harvest the strongest π–π stacking interaction, followed by those of analogs **2**, **24**, and eugenol. Docking results also reveal H-bonding potentials. The 1-OH groups of analogs **2**, **24**, **27**, and eugenol, which have been shown to be important for MAOA inhibition (see SAR section), are in H-bonding distance to the OH of Tyr197, the backbone O of Asn181, and/or the OH of Tyr444. Further, the 4-OH group of analog **27** is also in H-bonding distance to the carbonyl O of Gly443 and $N^{10}$ on the isoalloxazine ring. This additional H-bonding possibility, together with a stronger π–π stacking interaction, might explain the fact that even analog **27**, the smallest analog included in the study, is more potent MAOA inhibitor than eugenol (Table 2). SAR analysis has also shown that displacing the allyl function from the 4-position (as in eugenol) to the 6-position (as in analog **2**) increases potency for MAOA inhibition. Consistent with this result, docking and molecular modeling studies also predict stronger binding for analog **2** as its aromatic moiety is better positioned and oriented for a stronger π–π stacking interaction with the side chains of

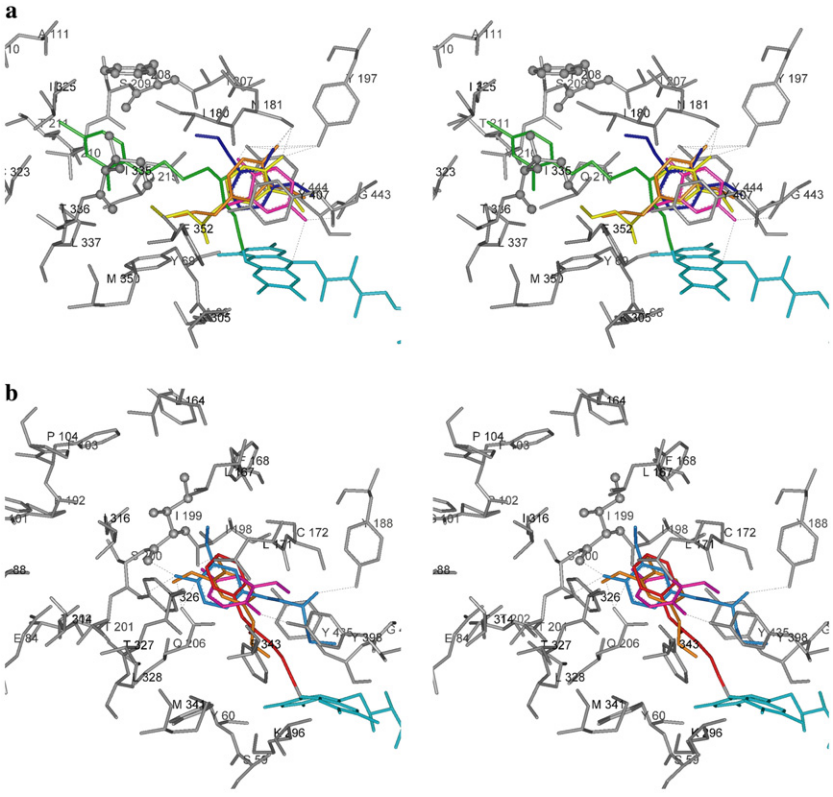


**Figure 6.** (a) Stereo views illustrating the calculated binding modes of eugenol, and the most potent MAOA inhibitory analogs superposed on the covalently bound clorgyline in MAOA. Color codes are clorgyline (green), eugenol (gold), analog **2** (blue), and analog **24** (yellow), and analog **27** (pink). Residues Phe208 and Ile335 are highlighted by ball-and-stick model for clarity. Both residues interact with clorgyline and are different from their corresponding residues (Ile199 and Tyr326) in MAOB. (b) Stereo views illustrating the calculated binding modes of eugenol and the most potent MAOB inhibitory analogs superposed on the covalently bound pargyline in MAOB. Color codes are pargyline (red), eugenol (gold), analog **27** (pink), and analog **29** (blue). Ile199 is highlighted by ball-and-stick model for clarity and for conformational comparison with the structures shown in Figure 7.

Tyr407 and Tyr444. Superposing the methoxyphenol ring of eugenol with that of analog **2** would bring its 4-allyl group too close to the isoalloxazine ring.

Curcumin (**10**) is the largest analog studied in this study. It is a symmetrical molecule with two 4-hydroxy-3-methoxyphenyl groups linked together by a relatively long and rigid linker 1,6-heptadiene-3,5-dione (Chart 1). It is a more potent MAOA inhibitor than eugenol (Table 2). Docking results show that one of its substituted phenols, such as that of eugenol, is sandwiched between the side chains of Tyr407 and Tyr444. The relative long linker, 1,6-heptadiene-3,5-dione, of curcumin extends its second substituted phenol into an area outlined by residues Phe208, Ile325, and Cys323, a pocket in which the 2,4-dichloro ring of clorgyline resides (result not shown).

### 2.8. Docking MAOB inhibitory analogs into the inhibitor-binding pocket of pargyline–MAOB

MAOB inhibitory analogs docked into the 'substrate cavity space' of the enzyme in a similar manner as pargyline, having their aromatic rings packed in between the side chains of Gln206 and Leu171. This mode of binding is illustrated in Figure 6b using two of the most potent analogs, **27** (pink) and **29** (blue). Docked eugenol molecule (gold) is also shown for comparison. That eugenol binds significantly weaker to MAOB than MAOA could be attributed to the lack of favorable π–π stacking interaction observed in MAOA. Except for curcumin and compound **29**, all MAOB inhibitory analogs avoid close contact with the phenolic side chains of Tyr398 and Tyr435 and the isoalloxazine ring. This phenomenon was also observed by Carrieri et al.[25] when they subjected a set of reversible and selective inhibitors of MAOB such as tetrazole and oxadiazolone, to a 3D QSAR study and flexible docking calculations.

### 2.9. Docking MAOB inhibitory analogs into the inhibitor-binding pocket of isatin–MAOB (1OJA) and 1,4-diphenyl-2-butene (1OJ9)

Docking pargyline into the inhibitor-binding pocket of pargyline–MAOB (1GOS) and that of isatin–MAOB (1OJA) yielded similar mode of binding (Figs. 4b and 7a). These results suggest that chemical manipulations leading to the formation of covalent pargyline–MAOB complex have not induced drastic changes to the active site conformation. The major structural difference between pargyline–MAOB and isatin–MAOB is that of Ile199.[15] In isatin–MAOB, the side chain of Ile199

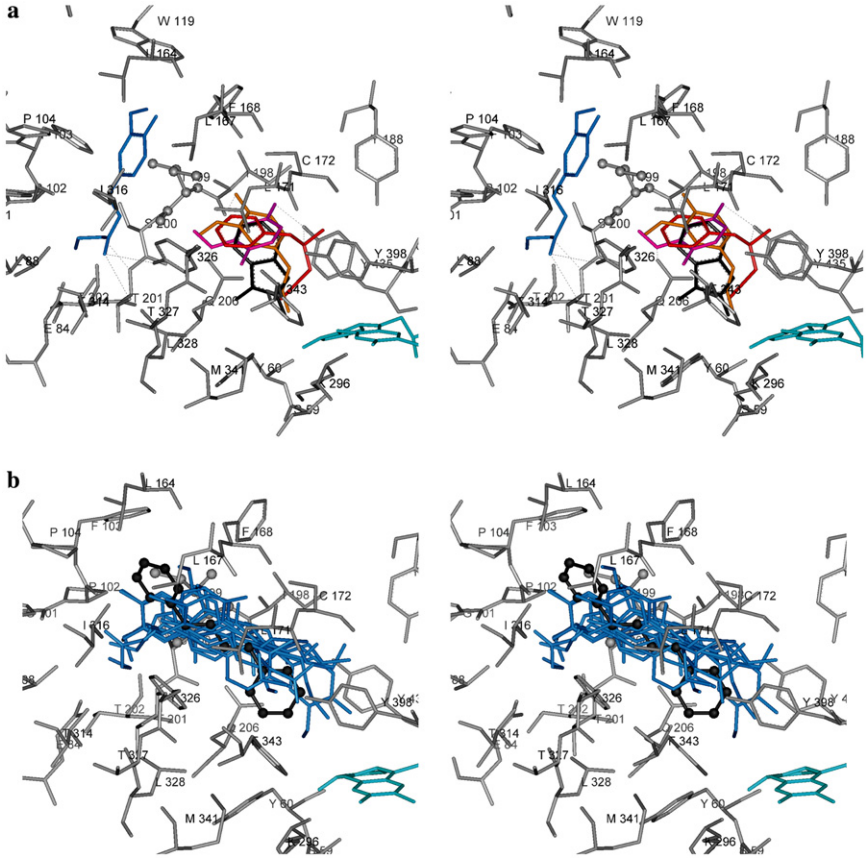


**Figure 7.** (a) Stereo views illustrating the calculated binding modes of pargyline, eugenol and the most potent MAOB inhibitory analogs superposed on reversibly bound Isatin (PDB code 1OJA). Color codes are pargyline (red), eugenol (gold), analog **27** (pink), analog **29** (blue), isatin (black, from crystal structure). Residue Ile199 is highlighted by ball-and-stick model for conformational comparison. (b) Stereo views illustrating the calculated binding modes of analog **29** superposed on reversibly bound 1,4-diphenyl-2-butene (PDB code 1OJ9). Color codes are analog **29** (blue) and 1,4-diphenyl-2-butene (black). Residue Ile199 is highlighted by ball-and-stick model for conformational comparison. 1,4-Diphenyl-2-butene is also highlighted by ball-and-stick model for clarity. Graphics were created using Insight II and docking was performed using AutoDock 3.0.[29]

assumes a 'closed' conformation that effectively separates the 'entrance cavity space' from the 'substrate cavity space' (Fig. 7a), whereas in pargyline–MAOB, the side chain of Ile199 is partially open to make room for the phenyl group of pargyline, as its acetylenic side chain established a covalent link with the isoalloxazine ring (Fig. 4a). Thus, one would expect that the closed 'substrate cavity space' of isatin–MAOB should be able to accommodate only small inhibitors such as eugenol. Indeed, docking eugenol, analog **27**, and isatin into the structure of isatin–MAOB placed these inhibitors inside the 'substrate cavity space' without any difficulty (Fig. 7a, gold and pink), whereas the larger inhibitor, analog **29**, was relocated to the 'entrance cavity space' (Fig. 7a, blue).

Crystallographic studies have shown that inhibitors with even larger sizes, such as 1,4-diphenyl-2-butene and lauryldimethylamine-*N*-oxide, bind to MAOB with an open conformation in which the 'entrance cavity space' and 'substrate cavity space' are fused into one.[15] Docking analog **29** into the fused binding pocket in 1,4-diphenylbutene-MAOB did not yield a single dominant mode of binding. Instead, the top ten binding modes are all different from one another (Fig. 7b) and with lowest docked energies range from −10.00 to −10.57 kcal/mol. Based on the data on hand, it is impossible to predict how and to which MAOB conformer does analog **29** bind. However, structural information obtained from the docking experiments (Fig. 7b) has provided a map useful for the future design of more potent and selective inhibitors for MAOB.

## 3. Conclusions

Eugenol inhibits both human MAOA and MAOB competitively with respect to their substrates 5-HT and DA. Between the two, MAOA is more sensitive. Eugenol analogs that inhibit MAOA also exhibit antidepressant-like action, whereas those that do not inhibit MAOA do not. This result suggests that the antidepressant-like action of eugenol could be mediated by its MAOA inhibitory activity. These findings provide for the first time a scientific rationale for the traditional use of RAG for the treatment of one of the most prevalent neuropsychiatric comorbidities of AD: depression. SAR studies revealed structural features important for MAOA and MAOB inhibition. This information, together with results obtained from docking and molecular modeling experiments, should be useful for future design of more potent and selective inhibitors for MAOA and MAOB.

## 4. Experimental

### 4.1. Chemicals

General chemicals were purchased from Sigma-Aldrich (St. Louis, MO) or VWR (Marlboro, MA). All organic solvents used were of AR grade and were supplied by J. P. Baker (Phillipsburg, NJ) or VWR. 4-Allyl-2-methoxyphenol (eugenol, **1**, 99% pure); 2-allyl-6-methoxyphenol (*o*-eugenol, **2**, 98%); 4-allyl-1,2-dimethoxybenzene (eugenol methyl ether, **3**, 99%); *trans*-2,4,5-trimethoxypropenylbenzene (β-asarone, **4**, 98%); *cis*-2,4,5-trimethoxypropenylbenzene (β-asarone, **5**, 70%); 2,4,5-trimethoxybenzoic acid (asaronic acid, **6**, 99%); 3,4,5-trimethoxybenzoic acid (**7**, 99%); 2,4,5-trimethoxycinnamic acid (**8**, 98%); 3,4-dihydroxycinnamic acid (**9**, 97%); 4-hydroxy-3-methoxyphenethyl alcohol (homovanillyl alcohol, **11**, 99%); 2-methoxyphenol (guaiacol, **16**, 98%); 2,6-dimethoxyphenol (**17**, 99%); 4-hydroxy-3-methoxybenzylamine HCl (**18**, 98%); 3-hydroxy-4-methoxybenzoic acid (**19**, 97%); 4-hydroxy-3-methoxyphenyl acetone (**20**, 96%); *trans*-3-hydroxy-4-methoxycinnamic acid (**21**, 97%); *trans*-4-hydroxy-3-methoxycinnamic acid (**22**, 99%); 2,3-dimethoxybenzoic acid (**23**, 99%); ethyl 4-hydroxy-3-methoxyphenylacetate (ethyl homovanillate, **24**, 97%); 4-hydroxy-3-methoxy-α-[methylaminomethyl] benzylalcohol HCl (methoxyhydroquinone, **27**, 98%); ethyl 4-hydroxy-3-methoxycinnamate (ethyl ferulate, **29**, 98%); metanephrine HCl (**31**, 99%); 3,4-dimethoxy-5-hydroxybenzaldehyde (**32**, 98%); 2,5-dimethoxybenzoic acid (**34**, 98%); 2-methoxybenzoic acid (*o*-anisic acid, **35**, 99%); 2,6-dimethoxybenzoic acid (**36**, 99%); 2,4-dimethoxyaniline (**37**, 97%); 2-methyl-5-methylaniline (**38**, 99%); 3-methoxyphenol (**39**, 96%); and 4-hydroxyphenylacetic acid (**40**, 98%) were purchased from Sigma-Aldrich, Inc. (St. Louis, MO). 1,7-Bis[4-hydroxy-3-methoxyphenyl]-1,6-heptadiene-3,5-dione (curcumin, **10**, 95%) was a product of Avocado Research Chemicals Ltd (Morecambe, UK). Purities of compounds used for MAO assays were over 99% and those selected for animal studies were at least 97%. When needed, commercial products were further purified on HPLC to achieve the required purities. All compounds were stored under argon in the dark.

Substrates used for MAOA (serotonin, 5-HT) and MAOB assays (dopamine, DA) were purchased from Sigma-Aldrich, Inc. The standard compounds of the products of MAOA and MAOB reactions, 5-hydroxyindole-3-acetaldehyde (5-HIAL) and 3,4-dihydroxyphenylacetaldehyde (DOPAL), respectively, were produced and purified in this laboratory by MAO-catalyzed oxidative deamination of 5-HT and DA, respectively, using purified rat liver mitochondrial membrane as the source of enzyme.[26] Human recombinant MAOA (M 7316, Lot 024K1057) and MAOB (M7441, Lot 053K0345) were purchased from Sigma-Aldrich, Inc.

### 4.2. MAOA and MAOB assays

MAOA and MAOB activities were determined using 5-HT and DA (10 μM unless otherwise specified) as the substrates, respectively, in TKK buffer (10 mM Tris–HCl, 10 mM KCl, and 10 mM KPi, pH 7.4) containing 0.4 mM sodium bisulfite with or without a specified concentration of eugenol or one of its structural analogs. To facilitate the dissolution of eugenol and its analogs, compounds were first dissolved in DMSO and diluted 500× in TKK buffer. The final concentration of DMSO in all enzyme assays was 0.2%. Owing to the low solubility of most of the compounds tested, the highest concentration for all compounds tested was 500 μM. Reactions were initiated by adding enzyme and were allowed to

proceed at 37 °C for 30 min. Reactions were stopped on ice and sample tubes were centrifuged at 4 °C in a Sorvall Microspin at top speed for 15 min. The reaction products, 5-HIAL and DOPAL, present in the supernatants as their stable bisulfite complexes, were liberated by diluting the supernatants 10- to 100-fold in 100 mM $NaPP_i$, pH 8.8, and analyzed by HPLC. Samples were analyzed within 4 h before degradation of 5-HIAL and DOPAL become significant. The amounts of enzymes added were adjusted so that not more than 5% of the substrates were converted into their respective aldehyde products. Inhibition potency was expressed as $IC_{50}$, a concentration at which a test compound reduces the initial enzyme reaction rate by 50%. The selectivity of inhibition for MAOA versus MAOB was defined as $[IC_{50}(MAOB)]/[IC_{50}(MAOA)]$.

### 4.3. HPLC analysis

The HPLC system for 5-HIAL and DOPAL analyses consisted of a BAS Sample Sentinel Autosampler with refrigerated sample compartment (set at 4 °C for all analyses), a PM80 solvent delivery system, and a LC-26 on-line degasser. The detector was a LC-4C amperometric controller with a CC-5 cross-flow thin-layer (0.005″) electrochemical cell composed of glassy carbon and silver/silver chloride reference electrode (Bioanalytical Systems, Inc., West Lafayette, IN). For routine analysis, the potential and sensitivity were set at 650 mV and 20 nA full scale, respectively. Column temperature was maintained at 30 °C with a Waters Temperature Control Module (Waters, Milford, MA). The aldehyde products 5-HIAL and DOPAL formed during MAOA and MAOB assays, respectively, were analyzed on a Beckman ultrasphere ODS, 5μ, $4.6 \times 250$ mm column. The column was developed at 30 °C at 1 ml/min in a mobile phase containing 3% methanol (v/v), 1% acetonitrile (v/v), 0.2 mM EDTA, and 0.1% TFA (v/v). Under this condition, the retention times for 5-HIAL and DA were 14.2, and 8.6 min, respectively. Data were collected and analyzed using a Waters Millennium-32, version 4.0 Chromatography Manager.

### 4.4. Animal experiments

Antidepressant-like activity of eugenol and three selected eugenol analogs was tested in CD-1 (ICR) mice using forced swim test (FST), an established antidepressant screening test.[27] CD-1 (ICR) mice (male, 6 weeks, BW: 28–30 g) were obtained from Japan SLC (Hamamatsu, Japan) and were housed 4 per cage in an animal facility maintained at 25 ± 1 °C on a 12/12 light/dark cycle (light on 07:00–19:00) with free access to food and distilled water. After 7 days of habituation, mice were divided into five groups, namely Group-vehicle control, -1, -19, -21, and -24. All test compounds were first dissolved in pure DMSO and then diluted 100× in distilled water and were administered as drinking water. Vehicle control animals received 1% DMSO. Drinks were prepared fresh everyday and given to the mice in light-protected drinking bottles. Dosages of the test compounds received by the mice were ≈0.17 mmol/day/kg body weight, calculated on the basis of their daily water intake. After 14 days of dosing, mice were subjected to the FST.

The FST was performed according to the procedure described previously with slight modifications.[13] Briefly, a WW-3002 apparatus (O'hara Co. Ltd, Tokyo, Japan) designed for mice was used in this experiment. The apparatus consists of a clear plastic water tank with a steel exercising wheel attached at water surface level and a clear cover on the top.[28] The tank was filled with fresh distilled water (25 °C). Mice placed in the water would swim toward the wheel and try to grab onto the ladders on the wheel. As a consequence, the wheel would rotate and the number of rotations was recorded automatically (1 rotation = 3 counts). When depressed, the mice would give up the struggle and stop grabbing, and hence stop turning the wheel. Each mouse was subjected to a pre-trial lasting 15 min and then a real trial the next day for 5 min (recorded).

All animal experiments were conducted according to the guideline approved by our institutes in compliance with the NIH Guide for Care and Use of Laboratory Animals. Every effort was made to minimize the number of animals used and any unnecessary anxiety or pain experienced by these animals.

### 4.5. Docking and molecular modeling

Crystal structures of all MAOs used for molecular docking were retrieved from the Protein Data Bank (PDB). Preparation of the protein PDBQS and ligand PDBQ files, calculations of grid maps, and molecular docking were performed using an automated docking method AutoDock program suite developed and validated by Morris et al.[29] The SYBYL MOL2 files of the structures of MAOs were created using Insight II and transformed to AutoDock-specific PDBQ files. Solvation parameters were added in accordance with Autodock 3.0 force field to create the PDBQS files. The SYBYL MOL2 files of the structures of eugenol analogs, and free clorgyline and pargyline were built using Insight II/Discover molecular modeling package. The AutoTors application of the AutoDock program suite was used to merge nonpolar hydrogen, initialize torsions for each compound, and transform the SYBYL MOL2 files to the PDBQ files. The 3D atomic affinity grid maps were computed for each atom type in the analog set, and an electrostatic grid map for the MAO model using AutoGrid 3.0 and the standard AutoDock 3.0 force field. The cubic grid with $60 \times 60 \times 60$ points and a spacing of 0.375 Å were centered at the enzyme active site that includes the 'substrate cavity space' and the 'entrance cavity space' defined by Binda et al.[15] The GA-LS method was adopted using the default settings. Docked structure with the lowest docked energy was selected and referred to as each analog's binding mode. The docked complexes and stereo views were created and inspected in Insight II program.

## Acknowledgments

This work was supported by the Endowment for Research in Human Biology, Inc. The continuous support by Dr. Bert L. Vallee is greatly appreciated.

## References and notes


1. St. George-Hyslop, P. H. *Biol. Psychiatry* **2000**, *47*, 183.
2. Selkoe, D. J. *Nature* **1999**, *399*, A23.
3. Evans, D. A.; Funkenstein, H. H.; Albert, M. S., et al. *JAMA* **1989**, *262*, 2251.
4. Evans, D. A. *Millbank Q.* **1990**, *68*, 267.
5. Bachurin, S. O. *Med. Res. Rev.* **2003**, *23*, 48.
6. Cutler, N. R.; Sramek, J. J. *Prog. NeuroPsychopharmacol. Biol. Psychiatry* **2001**, *25*, 27.
7. Pepeu, G. *Prog. NeuroPsychopharmacol. Biol. Psychiatry* **2001**, *25*, 193.
8. Irie, Y.; Keung, W. M. *Brain Res.* **2003**, *963*, 282.
9. Hardy, J.; Selkoe, D. J. *Science* **2002**, *297*, 353.
10. Lyketsos, C. G.; DelCampo, L.; Steinberg, M.; Miles, Q.; Steele, C. D.; Munro, V.; Baker, A. S.; Sheppard, J-M. E.; Frangakis, C.; Brandt, J.; Rabins, P. V. *Arch. Gen. Psychiatry* **2003**, *60*, 737.
11. Lyketsos, C. G.; Olin, J. *Biol. Psychiatry* **2002**, *52*, 243.
12. Olin, J. T.; Katz, I. R.; Meyers, B. S.; Schneider, L. S.; Lebowitz, B. D. *Am. J. Geriatr. Psychiatry* **2002**, *10*, 129.
13. Irie, Y.; Itokazu, N.; Anjiki, N.; Ishige, A.; Watanabe, K.; Keung, W. M. *Brain Res.* **2004**, *1011*, 243.
14. Binda, C.; Newton-Vinson, P.; Hubalek, F.; Edmondson, D. E.; Mattevi, A. *Nat. Struct. Biol.* **2002**, *9*, 22.
15. Binda, C.; Li, M.; Hubalek, F.; Nadia, R.; Edmondson, D. E.; Mattevi, A. *Proc. Natl. Acad. Sci. U.S.A.* **2003**, *100*, 9750.
16. Binda, C.; Hubalek, F.; Li, M.; Herzig, Y.; Sterling, J.; Edmondson, D. E.; Mattevi, A. *J. Med. Chem.* **2004**, *47*, 1767.
17. Ma, J.; Yoshimura, M.; Yamashita, E.; Nakagawa, A.; Ito, A.; Tsukihara, T. *J. Mol. Biol.* **2004**, *338*, 103.
18. Fowler, C.; Tipton, K. F. *J. Neurochem.* **1982**, *38*, 733.
19. Fowler, C.; Tipton, K. F. *J. Pharm. Pharmacol.* **1984**, *36*, 111.
20. Kong, L. D.; Cheng, C. H. K.; Tan, R. X. *J. Ethnopharmacol.* **2004**, *91*, 351.
21. Tsugeno, Y.; Ito, A. *J. Biol. Chem.* **1997**, *272*, 14033.
22. Geha, R. M.; Chen, K.; Shih, J. C. *J. Neurochem.* **2000**, *75*, 1304.
23. Fowler, C. J.; Oreland, L.; Callingham, B. A. *Pharm. Pharmacol.* **1981**, *33*, 341.
24. Dostert, P. L.; Benedetti, M. S.; Tipton, K. F. *Med. Res. Rev.* **1989**, *9*, 45.
25. Carrieri, A.; Carotti, A.; Barreca, M. L.; Altomare, C. *J. Comput. Mol. Des.* **2002**, *16*, 769.
26. Nilsson, G. E.; Tottmar, O. *J. Neurochem.* **1987**, *48*, 1566.
27. Prosolt, R. D.; Anton, G.; Blavet, N.; Jalfre, M. *Eur. J. Pharmacol.* **1978**, *47*, 379.
28. Nomura, S.; Shimizu, J.; Kinjo, M.; Kametani, H.; Nakawaza, T. *Eur. J. Pharmacol.* **1982**, *83*, 171.
29. Morris, G. M.; Goodsell, D. S.; Halliday, R. S.; Huey, R.; Hart, W. E.; Belew, R. K.; Olson, A. J. *J. Comput. Chem.* **1998**, *19*, 1639.